Automated Segmentation and Clinical Information on Dementia Diagnosis

A. Conci[1], A. Plastino[1], A. S. Souza[2], C. S. Kubrusly[3], D. M. Saade[4] and F. L. Seixa[1]

[1] UFF, Computer Institute, Passo da Patria 156, 24210 240 Niteroi, RJ, Brazil

[2] Radiology Department, LABS-Rede D´Or, 22032 011 Rio de Janeiro, RJ, Brazil

[3] PUC/RJ, Eletrical Engineering Department, R. Marques de S. Vicente 225
22453-900, Rio de Janeiro, RJ, Brazil

[4] UFF, Telecommunications Engineering Department, Passo da Patria 156
24210 240 Niteroi, RJ, Brazil

Abstract. This work intends to predict the clinical dementia rating (CDR) based on human brain volumetric segmentation measures from magnetic resonance (MR) images. These brain measures were extracted using an automated image segmentation method based on morphometry study and considering brain anatomical atlas. The prediction was achieved by Bayesian classifier. The classifier training was performed on 371 individuals from Open Access Series of Imaging Studies (OASIS) dataset. MR images and clinical information (including the Clinical Dementia Rating score) of each case are available on OASIS dataset. Experimentation results were assessed using true-positive rate. The final purpose of this work is to design a computer-aided diagnostic system that could be able to detect precociously neurodegenerative disorders, allowing early therapeutic interventions.

1 Introduction

Neurodegenerative disorders, such as multiple sclerosis, Alzheimer, Huntington and Parkinson diseases, are characterized by neuronal cell loss or dysfunction [1]. It is estimated that these disorders affect 11 million individuals, aged 60 years or older [1]. Alzheimer's disease (AD) represents the most common cause of dementia [2]. AD diagnostic criteria are based on the National Institute of Neurology Communicative Disorders and Stroke-Alzheimer's Disease and Related Disorders Association (NINCDS-ADRDA) criteria [3]. The Clinical Dementia Rating (CDR) scale is a global dementia staging instrument developed by the Memory and Aging Project [4]. CDR presents 5 scores: 0 (no dementia), 0.5 (questionable), 1 (mild), 2 (moderate) and 3 (severe). Agreement of CDR score with NINCDS-ADRDA's criteria achieves 86% for sensitivity and 100% for specificity [5]. A previous validation of this scale in Brazil was carried out achieving 91% sensitivity and 100% specificity [6]. Structures located in the medial temporal lobe, such as hippocampus and the parahippocampal

Conci A., Plastino A., Souza A., Kubrusly C., Saade D. and Seixas F. (2009).
Automated Segmentation and Clinical Information on Dementia Diagnosis.
In *Proceedings of the 1st International Workshop on Medical Image Analysis and Description for Diagnosis Systems*, pages 33-42
DOI: 10.5220/0001811200330042

gyrus are the first to manifest atrophy in AD [7]. Numerous studies and applications of brain volumetric measurements to early detect neurodegenerative disorders and to follow-up the patient disease progress have been presented [8]. It has been suggested that the atrophy of medial temporal lobe structures can predict AD risk [8]. These structures can be evaluated by magnetic resonance (MR) or, less accurately, computed tomography (CT) imaging. Our work proposes the use of automated segmentation methods and classifiers models to analyze brain structure volumes on MR images and predict patient's CDR scores. The automated segmentation algorithm is based on the Voxel-Based Morphometry (VBM) method [9]. The classifier model adopted was the naïve Bayesian approach [10], assuming that brain structure volume values are independent. 371 MR T1-weighted images from distinct patients, aged 18 to 96 years-old, were used in our practical experiments. This work extends the ideas presented in [11]. In next section the used segmentation procedure is presented. Section 3 considers the experiments and section 4 presents its conclusions.

2 Segmenting Brain Structures

Manual volumetric techniques are expensive and time-consuming. Some segmentation of medial temporal structures has being reported as taking about 75 minutes per exam and patient [12]. Moreover it results great variability of final medial temporal lobe volume [12-14]. Aiming to reduce the excessive time consumed and to standardize its volumetric acquisition method, decreasing inter and intra-personal volumes variability, automated image analyzing have been proposed [15]. This technique allows brain tissue segmentation and volume assessment without direct human intervention. Voxel-Based Morphometry (VBM) computes a customized template and the prior probability map from a population. The map was computed by segmenting the normalized images into grey matter (GM), white matter (WM) and cerebrum-spinal fluid (CSF), thus averaging the segmented image and finally obtaining the customized prior probability maps specific for GM, WM and CSF. Individual differences are handled computing spatially normalized mappings to the customized template [15].

Pennanen et al [16] applied VBM on 32 normal control subjects and 51 subjects with Mild Cognitive Impairment (MCI). They found a unilateral medial temporal atrophy in individuals with MCI, suggesting that these anatomical structures could be related to higher risk of AD. Ridha et al [17] compared the longitudinal volumetric MRI modifications with changes in performance on cognitive tests routinely used in AD clinical trials, observing strong correlations between brain atrophy, ventricular enlargement and Mini-Mental State Examination (MMSE) scores [18]. Jack et al [19] compared different MRI brain atrophy rate measures with clinical disease progression, studying normal elderly subjects, patients with MCI and patients with probable AD. Each subject underwent a brain MR examination at the time of the baseline clinical assessment and then again at the time of a follow-up clinical assessment, 1 to 5 years later. The results showed a strong correlation among hippocampus, entorhinal cortex, whole brain and ventricle volumes modification with MMSE, CDR and other cognitive tests. When referring brain medial temporal lobe structures segmentation, such works used manual segmentation [12-14]. In our work, such structures are seg-

mented in an automatic manner. This was achieved by using an anatomical atlas as following.

The brain anatomical structures segmentation method follows the sequence scheme shown in Fig. 1. Spatial normalization is an image registration method [20]. The registration problem consists of optimizing the parameters *q* from the affine matrix in order to minimize the objective function [20]. The objective function is composed by the sum of squared differences between the images, as shown in Equation 1. Some authors distinguish between different categories of alignments using the words registration, co-registration and normalization [20]. The term normalization is usually restricted to the inter subject registration situation, so we prefer to use the term spatial normalization. There are two steps in the spatial normalization process: (i) estimation of warp-field and (ii) application of warp-field with resample. The estimation of warp-field is made using an image similarity measurement (Equation 1). In order to perform normalization, a number of points in the template image are compared with points in the original image. The images might be scaled differently, so a scaling parameter denoted by *s* was included in the model:

$$\sum_i \left[f(M \cdot x_i) - s \cdot g(x_i) \right]^2 \tag{1}$$

where *M* is the affine[1] matrix defined by twelve parameters reproducing translation, rotation, zoom and shearing effects [21]. The optimization algorithm used is the Gauss-Newton based method [20]. Suppose that $b_i(q)$ is the function describing the difference between the original and template images at voxel *i,* when the vector of model parameters have values *q.* If the *q* parameters are decreased by *t,* Taylor's Theorem can be used to estimate the value of this difference:

$$b_i(q-t) \cong b_i(q) - t_1 \frac{\partial b_i(q)}{\partial q_1} - \ldots - t_{12} \frac{\partial b_i(q)}{\partial q_{12}} \tag{2}$$

Applying the Gauss-Newton optimization method, for iteration *n,* the *q* parameters are updated as:

$$q^{(n+1)} = q^n - (A^T \cdot A)^{-1} \cdot A^T \cdot b \tag{3}$$

where *A* is the matrix of the partial derivative coefficients. The iteration is repeated until the objective function can no longer be decreased or a maximum number of iterations is reached. A nonlinear spatial normalization is handled for correcting gross differences in head shapes that cannot be accounted by the affine normalization alone

[1] Observe that the term "afine" may have different meanings. Here it means a translation of an operator (e.g, of a square matrix). On the other hand, it is worth noticing that in the operator theory literature an afine transformation between normed spaces is a topological isomorphism (i.e., an invetible continuous linear transformation with a continuous inverse). A quasi afine transformation is an injective continuous linear transformation with a dense range. If a pair of operators are intertwined by an afine transformation, then they are said to be similar; if they are intertwined by a quasi afine transformation, then they are says to be quasi similar (see e.g.[21]).

.The nonlinear warps are modeled by linear combinations of smooth Discrete Cosine Transform (DCT) basis functions, considering a tri-dimensional space, as:

$$y_{li} = x_{li} + u_{li} = x_{li} + \sum_{j} q_{jl} d_j(x_i)$$

where $l=1,2,3$, q_{jk} is the j^{th} coefficient for dimension k and $d_j(x_i)$ is the j^{th} basis function at position x_i. The $d_j(x_i)$ is defined according to:

$$d_{1i} = \frac{1}{\sqrt{I}}; i = 1 \ldots I \quad and \quad d = \frac{\sqrt{2}}{\sqrt{I}} \cos\left(\frac{\pi(2i-1)(m-1)}{2I} \right); \forall i = 1 \ldots I, m = 2 \ldots M \qquad (4)$$

where d_{mi} is the mth coefficient, I is the set of voxels size. The objective function is:

$$\sum \left(f(y_i) - w \cdot g(x_i) \right)^2 \qquad (5)$$

where w is the scalar parameter, f the source image, g the template image. A linear regularization approach based upon Bayesian framework is used in order to avoid unnecessary deformations introducing instability. The segmentation method used an Expectation Maximization algorithm and a Gaussian mixture modeling. It assumes that each pixel belongs to a different class and pixel's intensities within each class is normal. A Bayesian model is used, where it is assumed that the modulation field U_{ij} has been drawn from a population for which the a priori probability distribution is known. It is assumed that the prior spatial probability of each pixel is Grey Matter (GM), White Matter (WM) or Cerebrum Spinal Fluid (CSF). The prior spatial probability images is provided by Montréal Neurological Institute (MNI) , as part of the International Consortium of Brain Mapping (ICBM) [22]. Suppose F_{ij} is the pixel's intensity of the original spatial normalized image, the probability of each voxel belonging to each class is assigned based on Bayes rules [11].

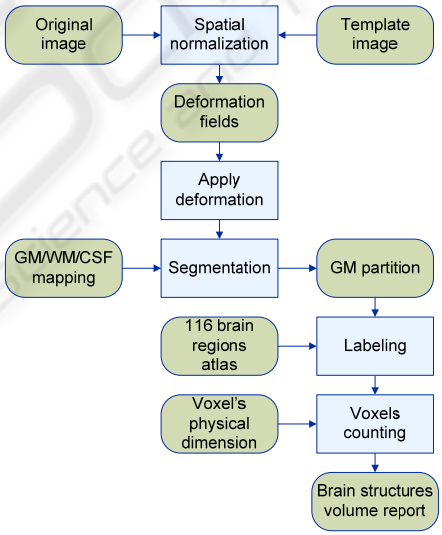

Fig. 1. Steps of the segmentation approach.

In the next step, each pixel belonging to gray matter is labeled based on MNI anatomical atlas constructed by manual segmentation, locating 116 brain structures defined by Broadman's areas [23]. Supposing the F_{ij} is the gray partition of the spatial normalized image and assuming that it is a binary image, the brain structure is obtained by logical operation as:

$$G_{ijk} = and(F_{ij}, B_{ijk}) \tag{6}$$

where G_{ijk} is the binary image representing each of brain structure coded by k Broadman areas and B_{ijk} is the anatomical atlas. The inverse deformation mapping is applied to bring back the labeled structures to the original space. Each brain structure volume is achieved by counting the pixels belonging to each Broadman area and multiplying them by its physical dimensions. Figure 2 shows the 3 brain tissues (GM, WM and CSF) segmented automatically by method described above.

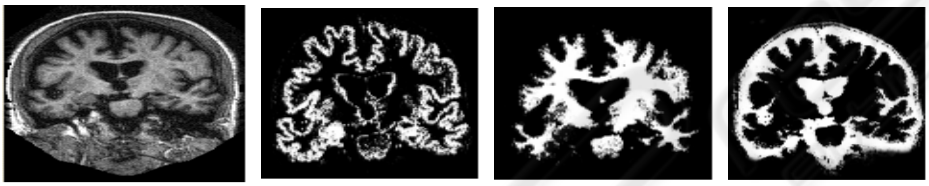

Fig. 2. Brain structures segmented: (a) original MR image; (b) WM; (c) GM; and (d) CSF.

2.1 Classification

Classification is a task of machine learning and data mining areas whose solution requires the construction of a classifier, that is, a function that assigns a class label to instances described by a set of attributes [24]. The induction of classifiers from data set of previous classified instances is a central problem in machine learning and data mining researches. The classification method adopted was the naïve Bayesian classifier [25]. The Bayesian classifier learns from training data the conditional probability of each attribute A_i given the class label C. Classification is done by applying Bayes rule to compute the probability of C given the particular instance of $A_1, \ldots, A_n$, and then predicting the class with the highest posterior probability. The patient clinical data set contains the brain structure volumes of each patient. These data are used as input for the classifier training. The continuous variables, such as the brain structure volumes, were transformed to a discrete number of intervals, reducing the number of values and improving Bayesian classifier performance [26]. The supervised discretization method performed was the Minimum Description Length (MDL) [27]. An attribute selection aiming to filter the most relevant attributes and to remove redundant data is applied. The attributes are evaluated using correlation-based feature selection (CFS) method of attribute subset selection [28] with "greedy hillclimbing" as search method. The naïve Bayesian classifier was trained and tested on a total of 371 instances and 138 attributes. Its performance was measured performing a cross-validation method using 10 folds [29].

3 Experiments and Text

The conducted experiments demonstrate the capability of predicting the CDR value using patient clinical data and brain structure volume information. 371 MR T1-weighted images from aged 18 to 96 years-old patients were used in the experiments. Images were downloaded from the OASIS (Open Access Series Imaging Studies) public database [30]. A number of 116 brain structures, including gray matter (GM), white matter (WM), cerebrospinal fluid (CSF) and whole brain, were segmented using the method described in Section 2. Patient data attributes such as age, gender, education, socioeconomic status, and MMSE were also considered. The CDR scale was selected as the attribute class. It was assumed a CDR scale ranging from 0 to 0.5 as normal control patient and ranging from 1 to 3 as patient in risk of dementia patient. Image processing and statistical analysis of structural T1 images were performed with SPM5 (Welcome Department of Imaging Neuroscience, University College London, visited 18/05/2008 http://www.fil.ion.ucl.ac.uk/spm). The classifier was performed with WEKA (http://www.cs.waikato.ac.nz/ml/weka; visited at April 16th, 2008). Table 1 and 2 show the patient CDR description grouped by aging and gender.

Table 1. CDR considering patient ages.

Ages	0.0	0.5	1.0	2.0	Total
0 to 20	16	0	0	0	16
20 to 40	126	0	0	0	126
40 to 60	59	0	0	0	59
60 to 80	52	36	16	0	104
Over 80	33	22	10	1	66
Total	286	58	26	1	371

Table 2. CDR considering patient gender.

Gender	0.0	0.5	1.0	2.0	Total
Female	112	25	8	1	146
Male	174	33	18	0	225
Total	286	58	26	1	371

The classifier training and tests were performed according to the criteria illustrated in Fig. 3. The criteria define the selected attributes and the set of instances following the combinations illustrated in Fig. 3, as well. The objective is to compare the classifier performance when using different datasets. The MMSE (Mini-Mental State Examination) is a brief questionnaire test used to assess cognition which is applied when patient has shown symptoms of cognitive deficit [18]. It is also used to predict the risk of dementia. The MMSE score and MRI volumetric measurements can be evaluated together, reaching a consensus diagnosis. In our experiment we performed the classifier's training with and without MMSE, because only a few patients had that information (166 missing values). The missing MMSE scores were replaced with modes from training data. Besides applying the supervised attribute selection method mentioned in Section 2.1, we also considered an attribute selection set based on medical knowl-

edge. The classifier performance was measured based on sensitivity or true-positive rate *(TPR$_C$)* for each class defined according to:

$$TPR_C = \frac{TP_C}{TP_C + FP_C} \tag{7}$$

where TP_C is the computing of true-positives (instances classified as class C that belong to class C) verified in test dataset; FP_C is the quantity of true-negatives is the computing of false-positives (instances classified as C but do not belong to class C). The classification results are summarized in Table 3, according to the selected criteria. We also considered in the experiments the patients with CDR equal to 0.5, because these patients represent a very mild dementia diagnostic state, requiring usually further information to identify a principle of cognitive deficit disorder. According to Table 3, we noticed that the best classifier performance was achieved by using selection criterion number 1 (including MMSE score and applying supervised attributes selection). Assuming medical knowledge, the best classifier performance was achieved by using selection criterion number 4.

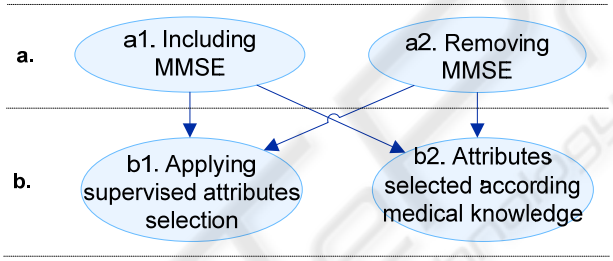

Fig. 3. Classifier training and tests strategy.

Table 3. Summarizing the results.

Selection	Criteria		TPR [%] 0.0³	TPR [%] >0³
1	a1	b1	90.4	96.3
2	a2	b1	88.4	96.3
3	a1	b2	89.5	88.9
4	a2	b2	86.9	92.6

The attributes selected by supervised attribute selection described in Section 2.1 are reported in Table 4 (line 1) sorted by highest to lowest relevance. The attributes selected by medical knowledge [31] are summarized in Table 4, as well. The attributes from patient dataset are described at Marcus *et al.* [30]. The remainding attributes are from automated brain structures segmentation algorithm described in Section 2, based on brain anatomical atlas describing the Broadman areas [31].

Table 4. Attributes used: [1] Patient data from OASIS dataset; [2] Brain tissues volumes normalized by total brain volume got from automated segmentation process; [3] Brain structures volume got from automated segmentation process; [4] The MMSE was used only in criterion set number 3.

N	Total	Attributes
1,2	14	MMSE[1][4], nWBV[1], VLiquor[2], nWhite[2], Supp_Motor_Area_L[2], Cingulum_Mid_L[2], Hippocampus_L[2], Hippocampus_R[2], ParaHippocampal_R[2], Cuneus_R[2], Angular_R[2], Caudate_L[2], Thalamus_L[2], Thamalus_R[2]
3,4	18	Gender[1], Age[1], Education[1], Socioeconomic status[1], MMSE[1][4], eTIV[1], nWBV[1], nGray[2], nWhite[2], nCSF[2], Cingulum_L[3], Cingulum_R[3], Hippocampus_L[3], Hippocampus_R[3], ParaHippocampal_L[3], ParaHippocampal_R[3], Amygdala_L[3], Amygdala_R[3]

Evaluating the 58 subjects with CDR equal to 0.5 (questionable dementia), 69% were classified as normal control and 31% as risk of dementia. It would be necessary to follow those subjects up, reviewing them two or three years later, in order to prediction accuracy. Fung *et al* [32] showed an AD patient classifier based on brain perfusion marker changing observed in SPECT imaging. Their classification approach was achieved by using SVM (support vector machines) [32].Concerning the results, they achieved a TPR equal to 86.7% for normal control subjects and 80% for subjects with AD. Devanand *et al* [33] conducted a longitudinal study performed in 139 patients with the objective of evaluating the utility of MRI hippocampal and entorhinal cortex atrophy in predicting conversion from mild cognitive impairment (MCI) to AD. Based on regression models [34] in the 3-year follow-up sample, they reached 80% specificity and 83.3% sensibility, using the attributes age, MMSE, SRT (Selective Reminding Test) delayed recall, WAIS-R (Wechlsler Adult Intelligence Scale-Revised), hippocampus and entorhinal cortex volumes. Fleisher *et al* [34] compared volumetric MRI of whole brain and medial temporal lobe structures to clinical measures for predicting progression from MCI to AD. They obtained a 78.8% predictive accuracy assuming hippocampus and ventricular volumes and cognitive measures, such as MMSE, ADAS (Alzheimer's Disease Assessment Scale), NYU recall test, Symbol Digit Modalities Test, etc.

4 Conclusions

This paper proposed a fully automated segmentation algorithm applied to dementia study. The paper showed also an application of a data mining method, in order to classify patients with risk of dementia based on volumes obtained on image processing. An advantage of using fully automated segmentation method should be standardizing brain structures volumetric assessment, allowing the patients with risk of incident AD could be followed up and treatment efficacy could be measured. As future work, we intend to apply the method into different image sets, associated to further clinical data, aiming to identify the risk of incidence AD in early stage.

References

1. M. Prince, "Dementia in developing countries: a consensus statement from the 10/66 Dementia Research Group," International Journal of Geriatric Psychiatry, vol. 15, pp. 14-20, 2000.
2. R. Nitrini, P. Caramelli, E. Herrera, V. S. Bahia, L. F. Caixeta, M. Radanovic, R. Anghinah, H. Charchat-Fichman, C. S. Porto, M. T. Carthery, A. P. J. Hartmann, N. Huang, J. Smid, E. P. Lima, L. T. Takada, and D. Y. Takahashi, "Incidence of dementia in a community-dwelling Brazilian population," Alzheimer Dis. Ass. Disorder, vol. 18, pp. 241-246, 2004.
3. G. McKhann, D. Drachman, M. Folstein, R. Katzman, D. Price, and E. M. Stadlan, "Clinical diagnosis of Alzheimer's disease: report of the NINCDS-ADRDA Workgroup under the auspices of Department of Health and Human Services Task Force on Alzheimer's Disease," Neurology, vol. 34, pp. 939-944, 1984.
4. C. P. Hughes, L. Berg, W. L. Danziger, L. A. Coben, and R. L. Martin, "A new clinical scale for the staging of dementia," British Journal of Psychiatry, vol. 140, pp. 566-572, 1982.
5. M. L. F. Chaves, A. L. Camozzato, C. Godinho, R. Kochhann, A. Schuh, V. L. d. Almeida, and J. Kaye, "Validity of the clinical dementia rating scale for the detection and staging of dementia in brazilian patients," Alzheimer Dis. Ass. Disorder, vol. 21, pp. 210-217, 2007.
6. M. B. M. M. Montaño and L. R. Ramos, "Validade da versão em português do clinical dementia rating," Revista de Saúde Pública, vol. 39, pp. 912-917, 2005.
7. R. C. Jack, R. C. Petersen, Y. C. Xu, S. C. Waring, P. C. O'Brien, E. G. Tangalos, G. E. Smith, R. J. Ivnik, and E. Kokmen, "Medial temporal atrophy on MRI in normal aging and very mild Alzheimer's disease," Neurology, vol. 49, pp. 786-794, 1997.
8. C. M. d. C. Bottino, "Morphometry through magnetic imaging," Revista de Saúde Pública, vol. 27, pp. 131-142, 2000.
9. J. Ashburner and K. J. Friston, "Voxel-based morphometry: the methods," Neuroimage, vol. 11, pp. 805-821, 2000.
10. G. John and P. Langley, "Estimating continuous distributions in bayesian classifiers," in Proc. Eleventh Conf. on Uncertainty in Artificial Intell., San Mateo, pp. 338-345 (1995)
11. F. L. Seixas, A. Souza, A. Plastino, D. Saade, and Aura Conci, "Clinical Dementia Rating Score Prediction Based on Automated Brain Image Segmentation", Intern. Worksh. on Biomedical and Health Informatics, IEEE Conference on Biomedical and Health Informatics - Philadelphia, PA, November 3-5, 2008.
12. R. L. Marchetti, C. M. C. Bottino, D. Azevedo, S. K. N. Marie, and C. C. d. Castro, "Confiabilidade de medidas volumétricas de estruturas temporais mesiais," Arquivos de Neuro-Psiquiatria, vol. 60, 2002.
13. C. R. Jack, C. K. Twomey, A. R. Zinsmeister, F. W. Sharbrough, R. C. Petersen, and G. D. Cascino, "Anterior temporal lobes and hippocampal formations: normative volumetric measurements from MR images in young adults," Radiology, vol. 172, pp. 549-554, 1989.
14. C. Watson, F. Andermann, and P. Gloor, "Anatomic basis of amygdaloid and hippocampal volume measurement by MR imaging," Neurology, vol. 42, pp. 1743-1750, 1992.
15. J. Ashburner and K. J. Friston, "Voxel-based morphometry - the methods," Neuroimage, vol. 11, pp. 805-821, 2000.
16. C. Pennanen, C. Testa, M. P. Laakso, M. Hallikainen, E. L. Helkala, T. Hänninen, M. Kivipelto, M. Könönen, A. Nissinen, S. Tervo, M. Vanhanen, R. Vanninen, G. B. Frisoni, and H. Soininen, "A voxel based morphometry study on mild cognitive impairment," Journal of Neurology, Neurosurgery Psychiatry, vol. 76, pp. 11-14, 2005.
17. B. H. Ridha, V. M. Anderson, J. Barnes, R. G. Boyes, S. L. Price, M. N. Rossor, J. L. Whitwell, L. Jenkins, R. S. Black, M. Grundman, and N. C. Fox, "Volumetric MRI and

cognitive measures in Alzheimer disease," Journal of Neurology, vol. 255, pp. 567-574, 2008.
18. M. F. Folstein, S. E. Folstein, and P. R. Hugh, "Mini-mental state: a practical method for grading the cognitive state of patients for the clinician," Psychiatry Research, vol. 12, pp. 189-198, 1975.
19. C. R. Jack, M. M. Shiung, J. L. Gunter, P. C. O'Brien, S. D. Weigand, D. S. Knopman, B. F. Boeve, R. J. Ivnik, G. E. Smith, R. H. Cha, E. G. Tangalos, and R. C. Petersen, "Comparison of different MRI brain atrophy rate measures with clinical disease progression in AD," Neurology, vol. 62, pp. 591-600, 2004.
20. D. L. G. Hill, P. G. Batchelor, M. Holden, and D. J. Hawkes, "Medical image registration," Physics in Medicine and Biology, vol. 46, pp. 1-45, 2001.
21. C. S. Kubrusly, Invariant subspaces and quasiaffine transforms of unitary operators, Progress in Nonlinear Differential Equations and their Applications, vol.42, pp.167--173, 2000.
22. A. C. Evans, D. L. Collins, S. R. Mills, E. D. Brown, R. L. Kelly, and T. M. Peters, "3D statistical neuroanatomical models from 305 MRI volumes," Proceedings IEEE-Nuclear Science Symposium and Medical Imaging Conference, pp. 1813-1817, 1993.
23. Y. Alemán-Gómez, L. Melie-García, and P. Valdés-Hernandez, "IBASPM: toolbox for automatic parcellation of brain structures," Neuroimage, vol. 27, 2006.
24. N. Friedman, D. Geiger, and M. Goldszmidt, "Bayesian network classifiers," Machine Learning, vol. 29, pp. 131-163, 1997.
25. R. O. Duda , P. E. Hart and D. G. Stork, Pattern classification. 2nd Ed. New York: John Wiley & Sons, 2001.
26. R. Abraham, B. Simha, and S. S. Ivengar, "A comparative analysis of discretization methods for medical datamining with Näive Bayesian classifier," in International Conference on Information Technology, pp. 235-236, 2006.
27. U. M. Fayyad and K. B. Irani, "Multi-interval discretization of continuous-valued attributes for classification learning," in Proceedings Thirteenth International Joint Conference on Artificial Intelligence, San Francisco, pp. 1022-1027, 1993.
28. M. A. Hall, "Correlation-based feature selection for machine learning," in Philosophy. vol. Doctor: University of Waikato, 1999.
29. J. Han and M. Kamber, Data mining: concepts and techniques, Morgan Kaufman, 2006.
30. D. S. Marcus, T. H. Wang, J. Parker, J. G. Csernansky, J. C. Morris, and R. L. Buckner, "Open access series of imaging studies (OASIS): cross-sectional MRI data in young, middle aged, nondemented and demented older adults," Journal of Cognitive Neuroscience, vol. 19, pp. 1498-1507, 2007.
31. A. S. d. Souza, "Espectroscopia de prótons na demência de Alzheimer e no comprometimento cognitivo," in Faculdade de Medicina. vol. Doctor: Universidade de São Paulo, (2005).
32. G. Fung and J. Stoeckel, "SVM feature selection for classification of SPECT images of Alzheimer's disease using spatial information," Knowledge and Information Systems, vol. 11, pp. 243-258, 2007.
33. D. P. Devanand, G. Pradhaban, X. Liu, A. Khandji, S. Santi, S. Segal, H. Rusinek, G. H. Pelton, L. S. Honig, R. Mayeux, Y. Stern, M. H. Tabert, and M. J. Leon, "Hippocampal and entorhinal atrophy in mild cognitive impairment," Neurology, vol. 68, pp. 828-836, 2007.
34. A. S. Fleisher, S. Sun, C. Taylor, C. P. Ward, A. C. Gamst, R. C. Petersen, C. R. Jack, P. S. Aisen, and L. J. Thal, "Volumetric MRI vs clinical predictors of Alzheimer disease in mild cognitive impairment," Neurology, vol. 70, pp. 191-199, 2008